

# Compact Circularly Polarized Crossed Dipole Antenna with Chip Inductors and Square Rings Loading for GPS Applications

Xiaojie Yang<sup>1, \*</sup>, Jiade Yuan<sup>1</sup>, and Guodong Han<sup>2</sup>

**Abstract**—A compact circularly polarized (CP) crossed dipole antenna with chip inductors and square rings loaded for Global Positioning System (GPS) is proposed in this letter. The CP radiation is produced by crossing two dipoles through a 90° phase delay line of a vacant-quarter printed ring. Four chip inductors inserted in the dipole arms and four square rings loaded at the back of the dipole arms are introduced to obtain a compact dipole size. The plane dimension of the proposed antenna is 28 mm × 28 mm, which can be widely used for GPS handheld devices. Details of the proposed antenna design and results are presented and discussed.

## 1. INTRODUCTION

Global Positioning System (GPS) is becoming more and more significant in human's daily life. Antennas play a vitally important role in GPS terminal equipment which requires antennas to satisfy specific performance conditions such as good circularly polarization (CP) property and wide 3 dB beamwidth. Various types of CP antennas have been chosen for GPS antennas, such as microstrip antennas [1–3] and quadrifilar helix antennas [4–6]. However, these configurations are generally bulky, which are not desirable for handheld devices.

In recent years, various types of compact crossed dipole antennas which can generate good CP radiation performance have been reported. In [7], different dipole lengths and phase delay metal strips are designed to generate two resonant modes for CP radiation. In [8], by introducing multiple near-field resonant parasitic elements, a CP planar crossed dipole antenna is implemented. In [9], crossed dipoles consist of a top-loaded triangular and a filleted rhombic to achieve the required input impedance relations for CP radiation. In [10–15], CP radiation is produced by crossing two dipoles through a 90° phase delay line of a vacant-quarter printed ring. Particularly in [15], the antenna employs insertion of meander lines in the dipole arms and shaping of the dipole arm end into arrowhead subtly to obtain a compact size for GPS application, whose plane dimension is 42 mm × 42 mm.

In this paper, a more compact CP crossed dipole antenna for GPS is proposed. The antenna is printed on both sides of a thin substrate, and a 90° phase delay line is used to generate the CP radiation mentioned in the abstract. The meander lines in the dipole arms are replaced by chip inductors, and four square rings are loaded at the back of the dipole arms, which are the methods to decrease the antenna size. Details of the antenna design and the experimental results for the antenna performance are presented and discussed.

## 2. ANTENNA DESIGN

Figure 1 shows the geometry of the proposed antenna. The antenna is composed of two printed dipoles and a plane reflector, which is fed by a 50 Ω coaxial feed line. The dipoles are designed on both sides of

---

*Received 19 November 2015, Accepted 11 December 2015, Scheduled 18 December 2015*

\* Corresponding author: Xiaojie Yang (yangxj900522@sina.com).

<sup>1</sup> College of Physics and Information Engineering, Fuzhou University, Fuzhou 350108, China. <sup>2</sup> The 54th Research Institute of CETC, Shijiazhuang, Hebei 050081, China.

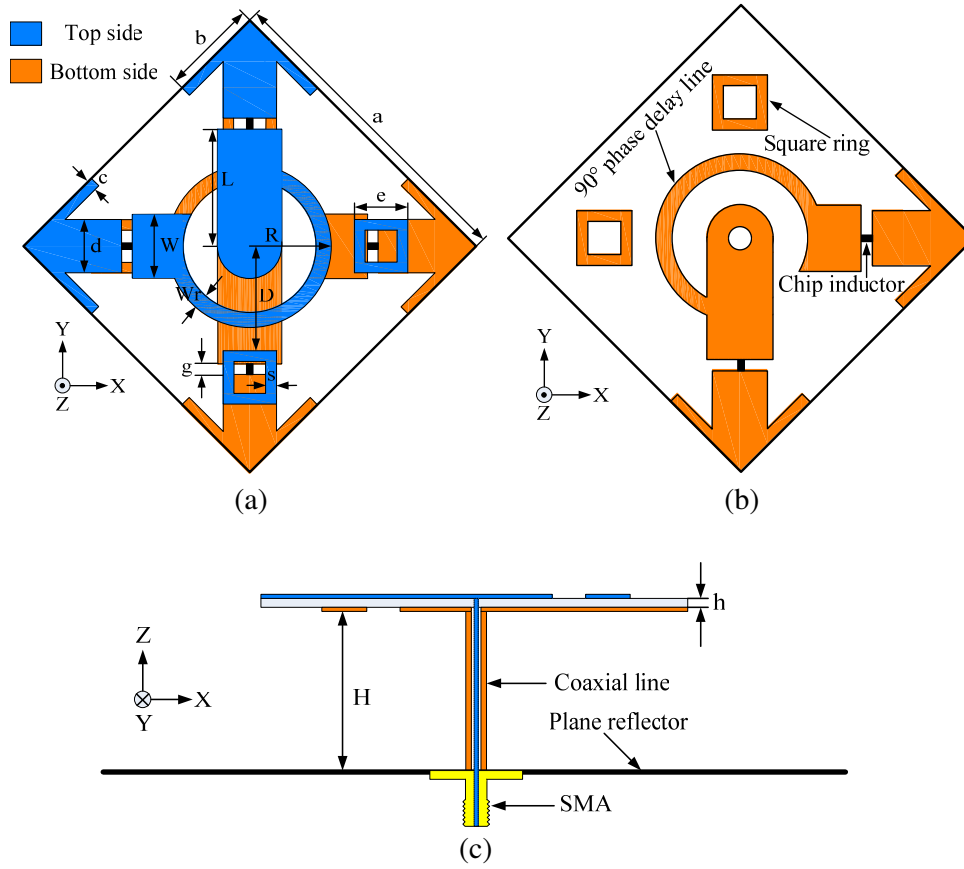


**Figure 1.** Geometry of the proposed antenna. (a) Top view, (b) top view of the bottom side, (c) side view with a plane reflector.

an FR4 substrate with dielectric constant 4.4, loss tangent 0.02, dimension  $28 \text{ mm} \times 28 \text{ mm}$  and thickness  $0.6 \text{ mm}$ . The thickness of the copper on each side of the FR4 substrate is  $35 \text{ }\mu\text{m}$ . The dimension of the plane reflector is  $85 \text{ mm} \times 85 \text{ mm}$ . The crossed dipoles are suspended at a height  $H$  from the top of the reflector. The inner conductor of the coaxial cable is extended through the substrate to feed the crossed arms at the top side of the substrate, and the outer conductor of the coaxial cable is welded to the crossed arms at the other side. Each dipole arm contains a chip inductor and an arrowhead shape end. Four square rings are loaded at the back of the dipole arms. The dipoles are crossed through a vacant-quarter printed ring which acts as the  $90^\circ$  phase delay line to realize CP radiation. The electromagnetic simulation software was used to investigate the characteristics of the antenna for a center frequency at  $1.575 \text{ GHz}$ . The optimized antenna design parameters are as follows:  $a = 28 \text{ mm}$ ,  $b = 9.5 \text{ mm}$ ,  $c = 1 \text{ mm}$ ,  $d = 5 \text{ mm}$ ,  $L = 11.1 \text{ mm}$ ,  $W = 6 \text{ mm}$ ,  $W_r = 1.8 \text{ mm}$ ,  $R = 8.2 \text{ mm}$ ,  $D = 11 \text{ mm}$ ,  $g = 0.8 \text{ mm}$ ,  $s = 1.1 \text{ mm}$ ,  $h = 0.6 \text{ mm}$ ,  $H = 30 \text{ mm}$ .

Figure 2(a) shows the process of antenna design. The initial design (design I) is similar to the antenna proposed in [15], whose dipole arm was inserted with meander lines and ended into an arrowhead shape. Then, four meander lines are replaced by four chip inductors (design II). Finally, four square rings are loaded at the back of the dipole arms (design III). All the designs use the same FR4 substrate with the dimension of  $28 \text{ mm} \times 28 \text{ mm}$  and thickness of  $0.6 \text{ mm}$ . The simulated  $S_{11}$  of the three designs are illustrated in Figure 2(b). It can be seen from Figure 2(b) that the resonant frequency would shift down from design I to design III with chip inductors and square rings additional loading. These results indicate that the compact size of the primary radiation elements at  $1.575 \text{ GHz}$  is attained by the use of chip inductors and square rings.

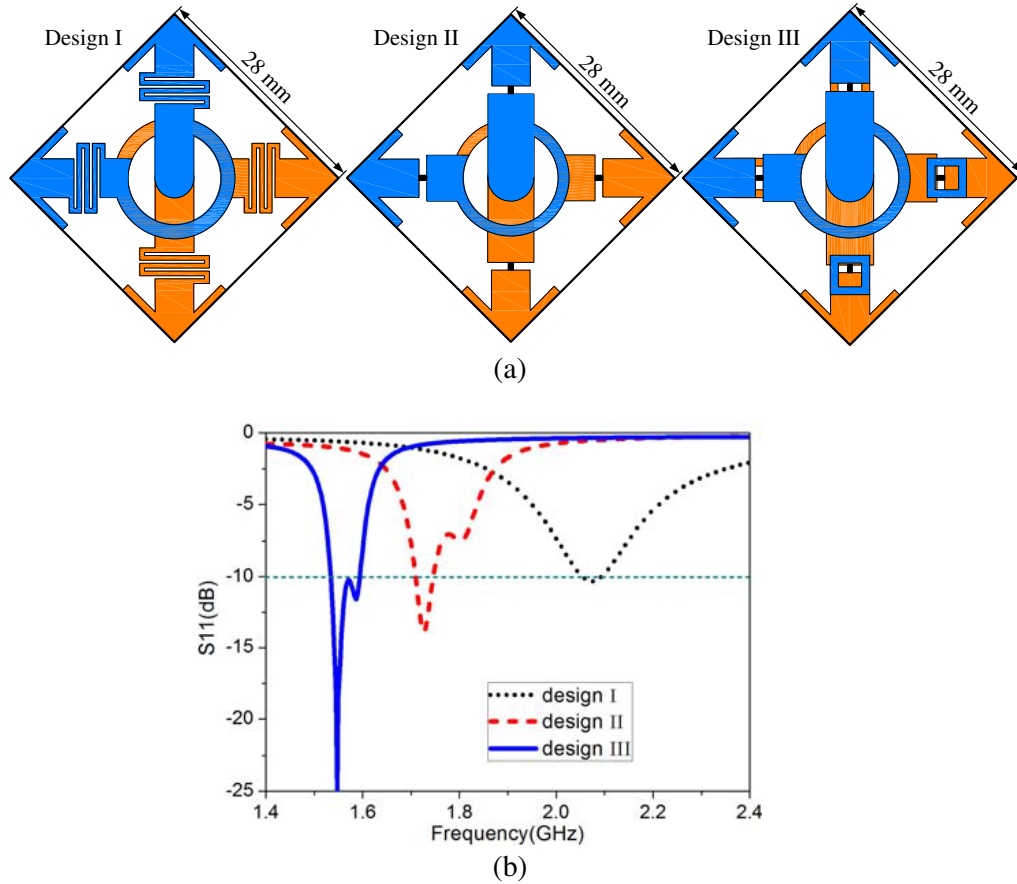


**Figure 2.** (a) Process of the dipole length reduction, (b)  $S_{11}$  for different antenna designs.

### 3. PARAMETRIC STUDY

As the chip inductors and square rings are the important parameters to affect the antenna size, the values of chip inductance  $L_i$ , square ring edge length  $e$  and square ring thickness  $s$  have been studied. Figure 3 shows simulated  $S_{11}$  and axial ratio (AR) with different values of  $L_i$ . As shown in Figures 3(a) and (b), with  $L_i$  varied from 9 nH to 11 nH in increments of 1 nH, the resonant and CP center frequencies decrease. (The CP center frequency here is defined as the frequency which has the minimum AR.) It means that properly increasing the value of  $L_i$  can reduce the dipole size, because inserting the inductors is equivalent to increasing the effective electric length of the antenna. It can also be known from Figure 3(b) that increasing the value of  $L_i$ , the 3 dB AR bandwidth shows almost no change because the AR bandwidth depends mainly upon the vacant-quarter printed ring. Figure 4 shows simulated  $S_{11}$  and AR with different values of  $e$ . It can be seen from Figures 4(a) and (b) that varying  $e$  from 4 mm to 6 mm with 1 mm step size, the center frequencies decrease. It means that properly increasing the square ring edge length can enhance the coupling capacitance between the square ring and the antenna, which can reduce the antenna size. Figure 4(b) also shows that the AR bandwidth is almost unchanged by changing the value of  $e$ . Figure 5 shows simulated  $S_{11}$  and AR with different values of  $s$ . As  $s$  is varied from 0.6 mm to 1.6 mm with increments of 0.5 mm, the resonance center frequencies decrease slightly, and the bandwidths also change slightly.

Figure 6 shows the simulated surface current distribution of the proposed antenna at 1.575 GHz for the two phase angles of  $0^\circ$  and  $90^\circ$ . It can be found from Figures 6(a) and (b) that the currents on the horizontally oriented dipole arms are very strong at the  $0^\circ$  phase angle, whereas the currents on the vertically oriented dipole arms are very strong at  $90^\circ$  phase angle. They show that the antenna has a good CP performance.

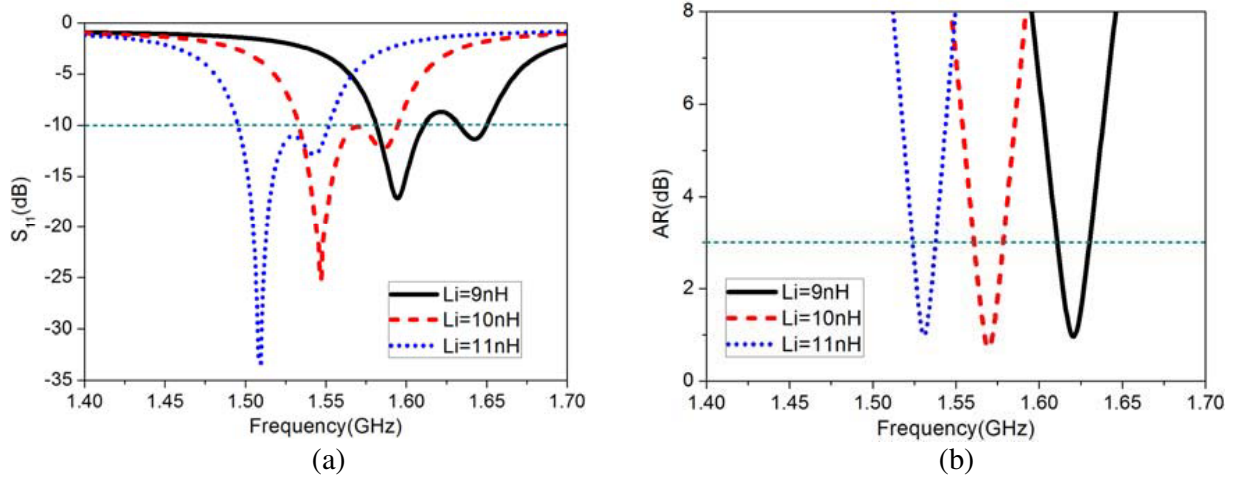


**Figure 3.** Simulated (a)  $S_{11}$  and (b) AR of the proposed antenna for various values of  $Li$ .

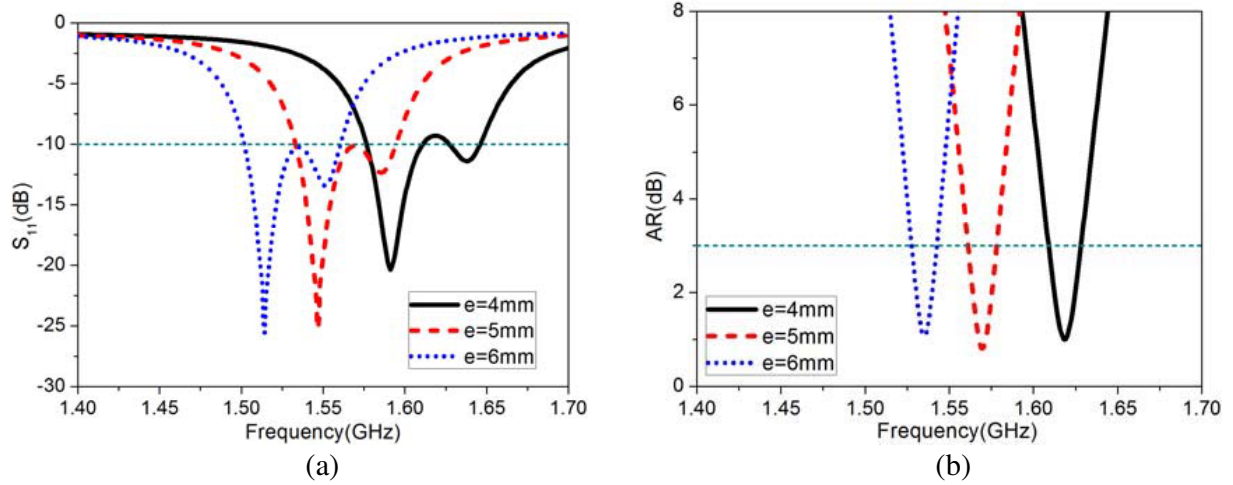


**Figure 4.** Simulated (a)  $S_{11}$  and (b) AR of the proposed antenna for various values of  $e$ .

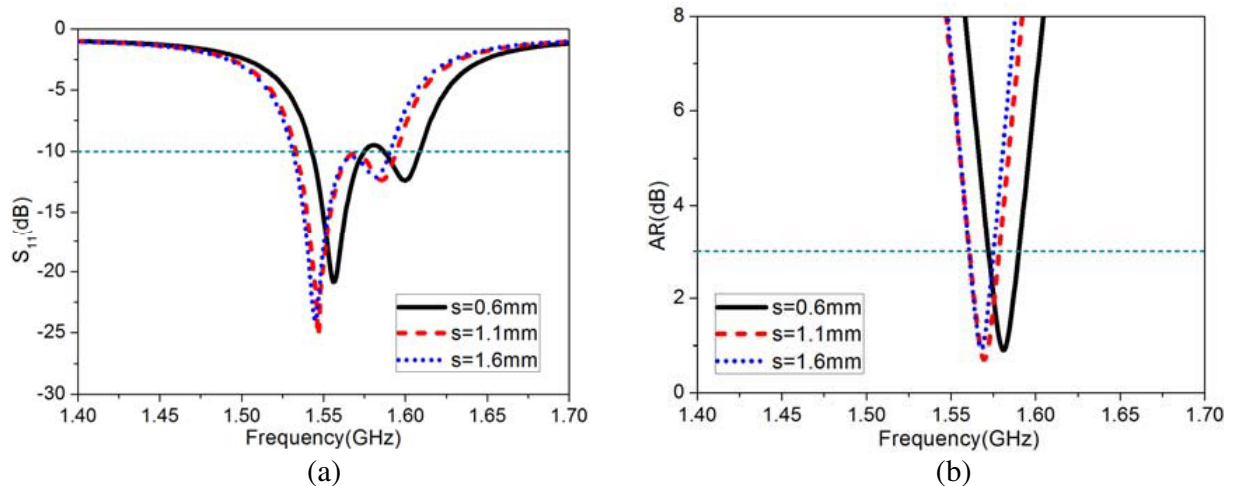


**Figure 5.** Simulated (a)  $S_{11}$  and (b) AR of the proposed antenna for various values of  $s$ .

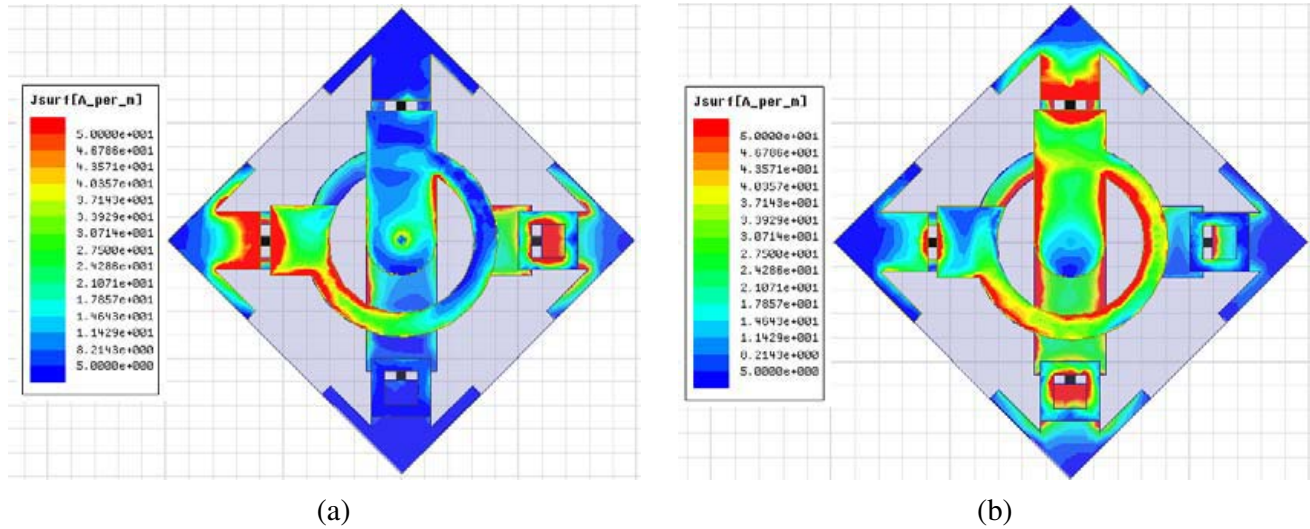


**Figure 6.** Simulated current distribution on the crossed dipoles at 1.575 GHz for (a) 0° and (b) 90° phase angles.

#### 4. MEASURED AND SIMULATED RESULTS

An FR4 substrate was used for fabricating the proposed crossed dipole antenna via a standard etching technology. The fabricated antenna is presented in Figure 7 which was used for input impedance and radiation pattern measurements. The measured and simulated  $S_{11}$  of the proposed antenna are shown in Figure 8. It can be observed that the measured bandwidth is 45 MHz (1.551–1.596 GHz) for  $S_{11} < -10$  dB, and the measured bandwidth is slightly smaller than the simulated one. The measured and simulated ARs of the proposed antenna are shown in Figure 9. The measured 3 dB AR bandwidth is 12 MHz (1.574–1.586 GHz) with a CP center frequency of 1.580 GHz. The measured CP center frequency is slightly higher than the simulated one. Figure 10 shows the measured and simulated radiation patterns of the antenna in the  $XOZ$  and  $YOZ$  planes at 1.575 GHz. The measurements yielded a gain of 2.7 dB and 3 dB beamwidths of 115° and 105° in the  $XOZ$  and  $YOZ$  planes, respectively. Due to the inevitable small fabrication errors and measuring errors, the measured and simulated results show small differences. However, the performance of the fabricated antenna satisfies the requirement of GPS applications.

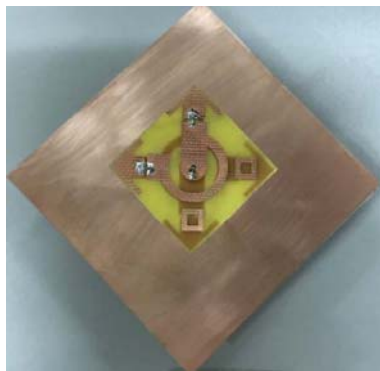


**Figure 7.** Implementation of the proposed antenna.

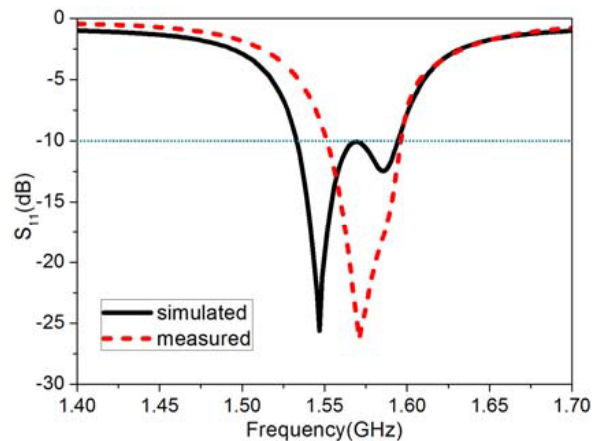


**Figure 8.** Measured and simulated  $S_{11}$  of the proposed antenna.

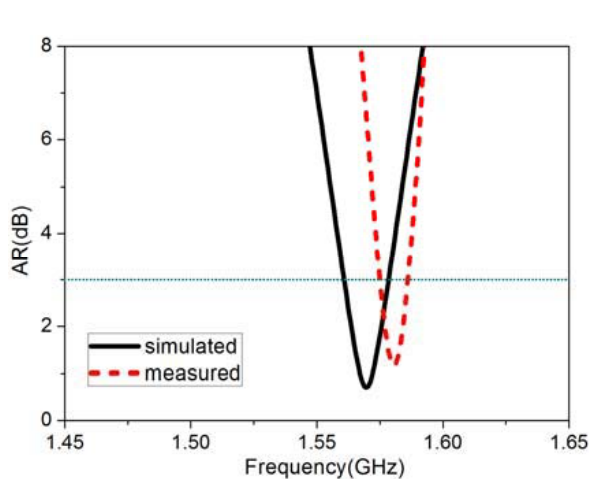


**Figure 9.** Measured and simulated AR of the proposed antenna.

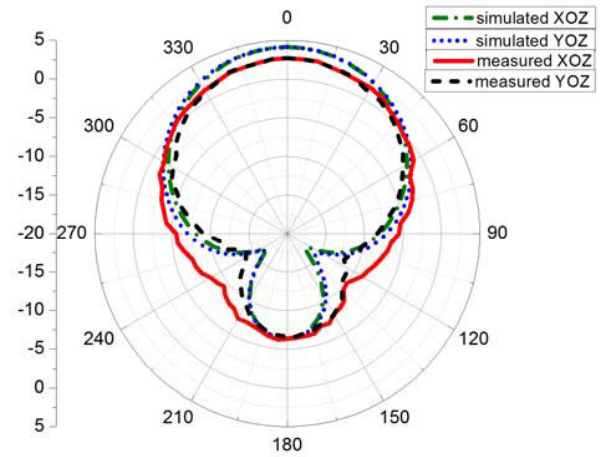


**Figure 10.** Measured and simulated radiation patterns of the proposed antenna at 1.575 GHz.

## 5. CONCLUSION

A compact crossed dipole antenna with a CP radiation for GPS is proposed. The compact size is due to the incorporation of four chip inductors and four square rings. The impedance bandwidth of the proposed antenna is 45 MHz (1.551–1.596 GHz) for  $S_{11} < -10$  dB; the 3 dB AR bandwidth is 12 MHz (1.574–1.586 GHz); the 3 dB beamwidths are  $115^\circ$  and  $105^\circ$  in the  $XOZ$  and  $YOZ$  planes, respectively. The proposed wide beamwidth antenna whose plane dimension is  $28 \text{ mm} \times 28 \text{ mm}$  can be widely applied to GPS purposes, especially in handheld devices.

## ACKNOWLEDGMENT

This work was supported by the Science and Technology Development Foundation of FuZhou University (2014-XQ-36) and Key Project of Industry, Education and Research of Fujian Province (2015H6014).

## REFERENCES

1. Ding, K., T. Yu, and Q. Zhang, "A compact stacked circularly polarized annular-ring microstrip antenna for GPS applications," *Progress In Electromagnetics Research Letters*, Vol. 40, 171–179, 2013.
2. Heidari, A. A., M. Heyrani, and M. Nakhkash, "A dual-band circularly polarized stub loaded microstrip patch antenna for GPS applications," *Progress In Electromagnetics Research*, Vol. 92, 195–208, 2009.
3. Labadie, N. R., S. K. Sharma, and G. M. Rebeiz, "A circularly polarized multiple radiating mode microstrip antenna for satellite receive applications," *IEEE Trans. Antennas Propagat.*, Vol. 62, No. 7, 3490–3500, 2014.
4. Wang, Y. S. and S. J. Chung, "A miniature quadrifilar helix antenna for global positioning satellite reception," *IEEE Trans. Antennas Propagat.*, Vol. 57, No. 12, 3746–3751, 2009.
5. Amin, M., R. Cahill, and V. Fusco, "Dual-mode compact structure comprising of side-fed bifilar and quadrifilar helix antenna," *IET Microw. Antennas Propag.*, Vol. 1, No. 5, 1006–1012, 2007.
6. Amin, M., J. Yousaf, and M. K. Amin, "Terrestrial mode quadrifilar helix antenna," *Progress In Electromagnetics Research Letters*, Vol. 27, 179–187, 2011.

7. Lin, Y. F., Y. K. Wang, H. M. Chen, and Z. Z. Yang, "Circularly polarized crossed dipole antenna with phase delay lines for RFID handheld reader," *IEEE Trans. Antennas Propagat.*, Vol. 60, No. 3, 1221–1227, 2012.
8. Jin, P. and R. W. Ziolkowski, "High-directivity, electrically small, low-profile near-field resonant parasitic antennas," *IEEE Antennas Wireless Propag. Lett.*, Vol. 11, 305–309, 2012.
9. Bai, X. and S.-W. Qu, "Wideband cavity-backed crossed dipoles for circularly polarization," *Progress In Electromagnetics Research Letters*, Vol. 36, 133–142, 2013.
10. Yoon, W. S., S. M. Han, J. W. Baik, S. Pyo, J. Lee, and Y. S. Kim, "Crossed dipole antenna with switchable circular polarisation sense," *Electron. Letters*, Vol. 45, No. 14, 717–718, 2009.
11. Baik, J. W., T. H. Lee, S. Pyo, S. M. Han, J. Jeong, and Y. S. Kim, "Broadband circularly polarized crossed dipole with parasitic loop resonators and its arrays," *IEEE Trans. Antennas Propagat.*, Vol. 59, No. 1, 80–88, 2011.
12. Chi, L.-P., S.-S. Bor, S.-M. Deng, C.-L. Tsai, P.-H. Juan, and K.-W. Liu, "A wideband wide-strip dipole antenna for circularly polarized wave operations," *Progress In Electromagnetics Research*, Vol. 100, 69–82, 2010.
13. Ta, S. X. and I. Park, "Crossed dipole loaded with magneto-electric dipole for wideband and wide-beam circularly polarized radiation," *IEEE Antennas Wireless Propag. Lett.*, Vol. 14, 358–361, 2015.
14. Ta, S. X., H. Choo, and I. Park, "Planar, and lightweight, circularly polarized crossed dipole antenna for handheld UHF RFID reader," *Microwave Opt. Technol. Lett.*, Vol. 55, No. 8, 1874–1878, 2013.
15. Ta, S. X., J. J. Han, and I. Park, "Compact circularly polarized composite cavity-backed crossed dipole for GPS applications," *Journal of Electromagnetic Engineering Science*, Vol. 13, No. 1, 44–49, 2013.